ELECTRONIC STRUCTURE OF BIAXIALLY STRAINED WURTZITE CRYSTALS GaN and AlN

J. A. MAJEWSKI, M. STÄDELE, and P. VOGL
Walter Schottky Institute, Technical University of Munich, D-85748 Garching, Germany

ABSTRACT

We present first-principles studies of the effect of biaxial (0001)-strain on the electronic structure of wurtzite GaN, and AlN. We provide accurate predictions of the valence band splittings as a function of strain, which may facilitate the interpretation of data from strained samples. The conduction and valence band effective mass tensors for AlN and GaN are also presented. The computed crystal-field and spin-orbit splittings in unstrained materials as well as the computed deformation potentials are in accord with available experimental data. We show that the numerically computed band energies can be excellently represented in terms of a 6-band $k \cdot p$ model. The present calculations are based on the first-principles pseudopotential method within the local-density formalism and include the spin-orbit interactions non-perturbatively.

INTRODUCTION

The group-III nitrides AlN, GaN, and InN have recently attracted much attention as candidates for short-wavelength optical devices [1]. The stable structure of bulk nitrides is the wurtzite structure. For these direct gap nitrides, the detailed knowledge of the carrier spectra in the vicinity of the center of the Brillouin zone is necessary for understanding and design of optoelectronic devices. Unfortunately, only little is known about the rather complex structure of the hole spectra. Additionally, the effect of strain on the electronic structure is appreciable due to the large lattice mismatch in nitride heterostructures.

In this paper, we provide quantitative *ab-initio* predictions of the electronic structure of group-III nitrides as a function of biaxial strain. The band structure near the band gap and the major optical transitions across the energy gap are calculated. We have determined the electron and hole effective mass tensors and the deformation potentials from our ab-initio calculations. These results permit us to determine the band parameters in terms of a 6x6 k·p Hamiltonian for the valence bands in the wurtzite structure.

The band structures of bulk AlN, GaN, and InN in the wurtzite and zincblende phase have been studied before extensively [2]. However, few reports have dealt with the details of the valence band edge and strain effects. First-principles calculations of the effect of biaxial strain on the electronic structure of the valence band edge in wurtzite nitrides have been recently presented [3, 4, 5]. Non-relativistic *ab-initio* calculations of the effective masses in AlN and GaN have been also performed [4, 6].

In the wurtzite structure, the top of the valence band at the Γ point consists of a doubly degenerate Γ_9 and two doubly degenerate Γ_7 states. In GaN, the separations between these states are of the order of 10 meV reflecting the comparable strength of the crystal field and spin-orbit interactions. The exciton energies corresponding to these split valence edge states have been recently measured in strained GaN films [7].

Employing the relativistic local density functional pseudopotential method and elasticity theory, we have analyzed the electronic band energies of three different wurtzite structure

Mat. Res. Soc. Symp. Proc. Vol. 449 © 1997 Materials Research Society

nitrides as a function of biaxial and hydrostatic strain. It turned out to be crucial to fully optimize internal structural parameters that are not determined by the symmetry, in order to ensure reliable and truly quantitative results.

THEORY

First-principles calculations

Our calculations are based on the first-principles total-energy pseudopotential method within the local-density-functional formalism [8]. We have used norm-conserving separable pseudopotentials [9, 10] and a preconditioned conjugate gradient algorithm [11] for minimizing the total crystal energy with respect to the electronic as well as the ionic degrees of freedom. These pseudopotentials are highly transferable, yet sufficiently soft so that a kinetic energy cutoff of 62 Ry suffices to yield converged total energies. We have used 14 special points [12] for the k-space integrations. The semicore Ga 3d-electrons are treated as part of the frozen core, but their considerable overlap with the valence electrons is accounted for by including the nonlinear core exchange-correlation correction [13]. This procedure yields lattice constants, atomic positions, and bulk moduli in very good agreement with experiment [5]. In order to realistically account for the interplay between strain and the spin-orbit interaction, we have taken into account relativistic effects nonperturbatively by using relativistic pseudopotentials. This method has been shown to predict spin-orbit splittings very reliably in other III-V compounds [14].

We have calculated the unstrained electronic band structures with the experimental lattice constants a_0 and c_0. This is known to yield valence band splittings in GaN that are in better agreement with experiment than those calculated at the self-consistently determined theoretical lattice constants [4]. The changes in lattice constants with strain are determined according to elasticity theory with experimental elastic constants [15, 16]. For a given in-plane lattice constant a, corresponding to the in-plane strain $\epsilon_{xx} = \epsilon_{yy} = a/a_0 - 1$, the lattice constant along the hexagonal axis is given by $c = c_0(1 + \alpha\epsilon_{xx})$, where $\alpha = -2c_{13}/c_{33}$ for biaxial strain, and $\alpha = (c_{11} + c_{12} - 2c_{13})/(c_{33} - c_{13})$ for hydrostatic pressure. The ϵ_{zz} strain component equals $\alpha\epsilon_{xx}$. Once the lattice constants are given, we have performed a full optimization of the atomic positions within the unit cell by calculating the Hellmann-Feynman forces. The latter determine the distance uc between cation and anion along the c-axis. This optimization of u has a significant influence on the valence band splittings [4, 5, 6].

Model 6 × 6 k · p Hamiltonian

The valence-band spectrum in the neigborhood of the band edge of wurtzite type materials can be reproduced by a 6 × 6 matrix $k \cdot p$ Hamiltonian that includes one Γ_9 and two Γ_7 band states [17, 18, 19]. This matrix also includes terms that are linear in the strain tensor. For biaxial or hydrostatic strain, these strain dependent matrix elements are proportional to four deformation potentials D_1, D_2, D_3, D_4. Three parameters Δ_1, Δ_2, and Δ_3 describe the splittings of the valence band maximum ($\mathbf{k} = 0$) and seven parameters $A_1 \ldots A_7$ determine the dispersions along different directions in the Brillouin Zone. In the present paper we use the definition of these valence band parameters and deformation potentials given in Ref. [19].

In the absence of the spin-orbit coupling, the Hamiltonian can be diagonalized analytically. For zero strain, the doubly degenerate energies of the valence band maximum are conventionally written as

$$E(\Gamma_9) = \frac{1}{3}\Delta_1 + \Delta_2 \,, \tag{1}$$

$$E(\Gamma_{7+}) = -\frac{1}{2}\left(\frac{\Delta_1}{3} + \Delta_2\right) + \sqrt{\left(\frac{\Delta_1 - \Delta_2}{2}\right)^2 + 2\Delta_3^2} \,, \tag{2}$$

$$E(\Gamma_{7-}) = -\frac{1}{2}\left(\frac{\Delta_1}{3} + \Delta_2\right) - \sqrt{\left(\frac{\Delta_1 - \Delta_2}{2}\right)^2 + 2\Delta_3^2} \,. \tag{3}$$

The constants Δ_2 and Δ_3 are spin-orbit Hamiltonian matrix elements, whereas Δ_1 is conventionally termed crystal-field splitting. When $\Delta_1 > 0$, as is the case in GaN and InN [5, 18], the ordering of these band states is $\Gamma_{7-} < \Gamma_{7+} < \Gamma_9$. For $\Delta_1 < 0$, which is the case for AlN [5, 18], the states form the sequence $\Gamma_{7-} < \Gamma_9 < \Gamma_{7+}$. The Γ_9 state is always termed heavy-hole (hh) state and the energy below forms the light-hole state (lh). This is Γ_{7+} for GaN, and InN and Γ_{7-} for AlN. The third eigenvalue defines the crystal field split-off state (cs). These definitions are kept for $\mathbf{k} \neq 0$.

The shift of the conduction band edge at Γ-point with strain and the band dispersion in the vicinity of this point is governed by two deformation potentials D_{1c} , and D_{2c} and two effective masses ($m_e^{\parallel}$ and $m_e^{\perp}$), respectively,

$$E_c(\mathbf{k}) = E_c(0) + \frac{\hbar^2 k_z^2}{2m_e^{\parallel}} + \frac{\hbar^2(k_x^2 + k_y^2)}{2m_e^{\perp}} + D_{1c}\epsilon_{zz} + D_{2c}(\epsilon_{xx} + \epsilon_{xx}) \,. \tag{4}$$

We measure this strain dependence relative to the center of gravity of the valence band.

RESULTS

Effective masses and valence band splittings

For unstrained wurtzite GaN, the present ab-initio calculations predict $E_{hh}(\Gamma_9)$ - $E_{lh}(\Gamma_{7+})$ = 6.8 meV (6 meV [20], [21], [22]) and $E_{hh}(\Gamma_9)$ - $E_{cs}(\Gamma_{7-})$ = 33.7 meV (28meV [21], 25meV [22], 23meV [20]) in fair agreement with experimental data (given in parenthesis) of bulk GaN and epitaxial GaN films that are believed to be strain free. In InN, the $hh - lh$ and $hh - cs$ splittings are predicted to be 5 meV and 34 meV, respectively. In AlN, $E_{cs}(\Gamma_{7+})$ forms the top of the valence band, and the calculations yield the $cs - hh$ and $hh - lh$ splitting to be equal to 212 meV and 14 meV, respectively.

The calculated components of the effective mass tensor at Γ for electrons and holes in AlN and GaN are given in Table I.

Table I. Electron and hole effective masses (in units of m_0)

	$m_e^{\parallel}$	$m_e^{\perp}$	$m_{hh}^{\parallel}$	$m_{hh}^{\perp}$	$m_{lh}^{\parallel}$	$m_{lh}^{\perp}$	$m_{cs}^{\parallel}$	$m_{cs}^{\perp}$
AlN	0.32	0.33	3.52	0.73	3.44	0.73	0.26	4.49
GaN	0.18	0.20	2.09	0.37	0.74	0.39	0.18	0.94

The masses were calculated by numerical differentiation of the dispersion relations obtained from the present relativistic *ab-initio* calculations. The calculated conduction band masses

for GaN are in good agreement with recent optically detected cyclotron resonance data [23] that givea polaron mass of $0.22m_0$. The corresponding bare mass is estimated to be $0.20m_0$ [23]. We are not aware of experimental data on the valence band effective masses in nitrides. The predicted hole masses show a strong anisotropy. We have excluded the calculated masses of InN from Table I since the LDA calculations grossly underestimate the energy gap of wurtzite InN (it is only 0.1 eV) and are therefore unlikely to yield reliable masses.

Biaxial strain effects

Very recently, free exciton lines at Γ have been measured in epitaxial GaN films. In the same samples, the amount of strain could be directly measured by X-rays [7]. These data allow us to directly compare theory with experiment, as depicted in Fig. 1. We have increased all valence to conduction band transition energies by a rigid, strain-independent self energy of 1.209 eV. In this way, the calculated *hh* to conduction-band transition energy for zero pressure coincides with the observed exciton transition energy of 3.4745 eV measured for bulk GaN [21]. Fig. 1 shows excellent agreement between theory and experiment for all other transition energies. This may help to determine the actual strain in epitaxial films from the measured optical excitonic spectra. We notice that for a tensile strain of about 0.2% the light-hole band becomes the top of the valence band.

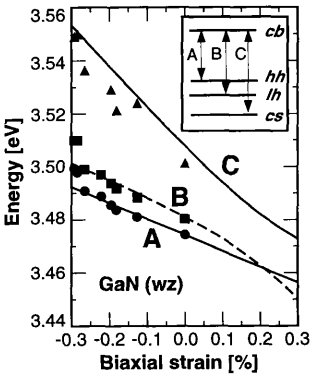

Figure 1: Comparison of experimental free exciton energies of strained GaN from Ref. 7, and unstrained GaN [21] (full dots, squares, and triangles denote energies of A, B, and C exciton lines, respectively) with present theoretical calculations (lines). The theoretically calculated energies were rigidly shifted by 1.209 eV. This energy shift includes the self-energy correction to the LDA gaps and the exciton binding energy.

Valence band parameters and deformation potentials

From the calculated band structures, we have determined all parameters in the 6×6 $k \cdot p$ Hamiltonian, following the notation of Ref.[19]. In order to determine Δ_1 independently from Δ_2 and Δ_3, we have also performed nonrelativistic calculations. From the relativistic bands, we can deduce Δ_2 and Δ_3. The parameters $A_1 \ldots A_5$ can easily be determined from the effective masses parallel and transverse to the hexagonal axis. Since the masses are independent of A_6, it is difficult to determine this parameter from the eigenvalues at small $\mathbf{k}$. Therefore, we have used the quasicubic model that gives $A_6 = (A_3 + 4A_5)/\sqrt{2}$. Finally, A_7 can be determined from the spin splittings of the bands along the direction orthogonal to the hexagonal axis. In order to determine the valence (D_3 and D_4) and conduction deformation

potentials (D_{1c} and D_{2c}), we have computed the derivative $(dE_i/d\epsilon_{xx})|_{\epsilon=0}$, i = valence and conduction band, for two different strain tensors.

The complete sets of $k \cdot p$ parameters for AlN and GaN are summarized in Tables II. The conduction band deformation potentials D_{1c} and D_{2c} are equal to -10.23 eV and -9.65 eV for AlN, and -9.47 eV, -7.17 eV for GaN, respectively.

Table II. Valence band parameters of the 6 × 6 k · p model for AlN and GaN. Δ_1, Δ_2, and Δ_3 are given in meV, all other parameters in eV.

	Δ_1	Δ_2	Δ_3	A_1	A_2	A_3	A_4	A_5	A_6	A_7	D_3	D_4
AlN	-219	6.6	6.7	-3.82	-0.22	3.54	-1.16	-1.33	-1.25	0.00	9.02	-3.99
GaN	24	5.4	6.8	-6.40	-0.80	5.93	-1.96	-2.32	-3.02	-0.026	6.26	-3.29

In Fig. 2, we depict the calculated valence band edge structure of wurtzite GaN perpendicular to the hexagonal axis ($\Gamma \rightarrow M$) for three different biaxial strains. The discrepancies between the full diagonalization of the Hamiltonian and the 6-band $k \cdot p$ model are negligible up to wave vectors of the order of 0.15 Å^{-1}.

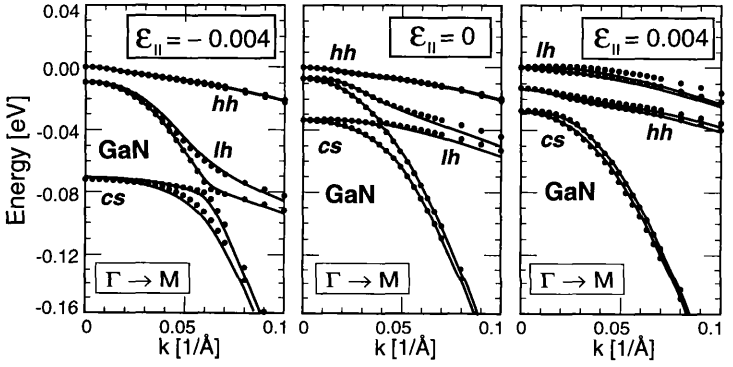

Figure 2: Valence-band dispersions along the transverse axes for biaxially strained and unstrained wurtzite GaN. The full dots denote the present *ab-initio* results, whereas the lines represent the solutions of the 6 × 6 $k \cdot p$ model Hamiltonian with the parameters from Table II.

CONCLUSIONS

In summary, we have predicted the hole effective mass tensor for AlN and GaN. We have determined the parameters of 6-band model Hamiltonian that very accurately reproduces the hole spectra near the valence band edge in biaxially strained AlN and GaN.

ACKNOWLEDGMENTS

This work was supported by the Bayerische Forschungsverbund FOROPTO and the Deutsche Forschungsgemeinschaft, project SFB 348.

REFERENCES

1. S. Strite and H. Morkoç, J. Vac. Sci. Technol. B **10**, 1237 (1992).

2. For a review see, J. H. Edgar editor, *Properties of Group III Nitrides* (Electronic Materials Information Service (EMIS), London, 1994).

3. K. Kim, W. R. L. Lambrecht, and B. Segall, Phys. Rev. B **53**, 16310 (1996).

4. W. R. L. Lambrecht, K. Kim, S. N. Rashkeev, and B. Segall, Mater. Res. Soc. Symp. Proc. **395**, 455 (1996).

5. J. A. Majewski, M. Städele, and P. Vogl, MRS Internet J. Nitride Semicond. Res. **1**, 30 (1996).

6. M. Suzuki, T. Uenoyama, and A. Yanase, Phys. Rev. B **52**, 8132 (1995).

7. S. Chichibu, A. Shikanai, T. Azuhata, T. Sota, A. Kuramata, K. Horino, and S. Nakamura, Appl. Phys. Lett. **68**, 3766 (1996).

8. W. E. Pickett, Comp. Phys. Rep. **9** 115 (1989).

9. N. Troullier and J. L. Martins, Phys. Rev. B **43**, 1993 (1991).

10. L. Kleinman and D. M. Bylander, Phys. Rev. Lett. **48**, 1425 (1982).

11. M. C. Payne, M. P. Teter, D. C. Allan, T. A. Arias, and J. D. Joannopoulos, Rev. Mod. Phys. **64**, 1045 (1992).

12. P. J. H. Denteneer and W. Van Haeringen, Sol. State Commun. **59**, 829 (1986).

13. S. G. Louie, S. Froyen, and M. L. Cohen, Phys. Rev. B **26**, 1738 (1982).

14. J. A. Majewski, in *The Physics of Semiconductors*, Ed. D. J. Lockwood (World Scientific, Singapore, 1995) pp. 711-714.

15. A. Polian, M. Grimsditch, and I. Grzegory, J. Appl. Phys. **79**, 3343 (1996).

16. L. E. Neil, M. Grimsditch, and R. H. French, J. Am. Ceram. Soc. **76**, 1132 (1993).

17. G. L. Bir and G. E. Pikus, *Symmetry and strain-induced effects in Semiconductors* (John Wiley & Sons, New York, 1974), p. 1111.

18. Y. M. Sirenko, J.-B. Jeon, K. W. Kim, M. A. Littlejohn, and M. A. Stroscio, Phys. Rev. B **53**, 1997 (1996).

19. S. L. Chuang and C. S. Chang, Phys. Rev. B **54**, 2491 (1996).

20. D. Volm, K. Oettinger, T. Streibl, D. Kovalev, M. Ben-Chorin, J. Diener, B. K. Meyer, J. Majewski, L. Eckey, A. Hoffmann, H. Amano, K. Hiramatsu, and D. Detchprohm, Phys. Rev. B **53**, 16543 (1996).

21. R. Dingle, D. D. Sell, S. E. Stokowski, and M. Ilegems, Phys. Rev. B **4**, 1211 (1971).

22. B. Monemar, Phys. Rev. B **10**, 676 (1974).

23. M. Drechsler, B. K. Meyer, D. M. Hoffmann, D. Detchprohm, H. Amano, and I. Akasaki, Jpn. J. Appl. Phys. **34**, L1178 (1995).